DONG THAP UNIVERSITY JOURNAL OF SCIENCE
Tạp chí Khoa học Đại học Đồng Tháp
Natural Sciences Issue
ISSN 0866-7675 | e-ISSN 2815-567X

DOI: https://doi.org/10.52714/dthu.ns.2281.1828

ELECTRONIC STATES OF SILICENE UNDER NON-UNIFORM MAGNETIC FIELD

Vo Thi Anh Thu[1], Dao Trong Tien[1], Nguyen Thanh Tam[1], and Huynh Vinh Phuc[2]*

[1]Student, Faculty of Natural Sciences Teacher Education, School of Education, Dong Thap University, Cao Lanh 870000, Vietnam

[2]Faculty of Natural Sciences Teacher Education, School of Education, Dong Thap University, Cao Lanh 870000, Vietnam

**Corresponding author, Email: hvphuc@dthu.edu.vn*

Article history

Received: 31/3/2025; Received in revised form: 12/4/2025; Accepted: 14/4/2025

Abstract

In this study, we investigate the electronic states according to the single-particle model of silicene under an exponentially decaying magnetic field. By solving the Dirac-Weyl equations, we derive exact expressions for the wave functions and the corresponding Landau level spectrum. We also examine in detail the effects of the electric field, the Zeeman effect, and the non-uniform magnetic field on the probability density and current distributions. Furthermore, we compare our results with those of graphene in the presence of a non-uniform magnetic field.

Keywords: *Dirac-Weyl equations, exponentially decaying magnetic field, Silicene.*

Cite: Huynh, V. P., Vo, T. A. T., Dao, T. T., & Nguyen, T. T. Electronic properties of silicene under non-uniform magnetic field. *Dong Thap University Journal of Science, 15*(5), 1-10. https://doi.org/10.52714/dthu.ns.2281.1828
Copyright © 2026 The author(s). This work is licensed under a CC BY-NC 4.0 License.

TRẠNG THÁI ĐIỆN TỬ CỦA HỆ SILICENE TRONG TỪ TRƯỜNG KHÔNG ĐỀU

Võ Thị Anh Thư[1], Đào Trọng Tiến[1], Nguyễn Thành Tâm[1] và Huỳnh Vĩnh Phúc[2*]

[1]Sinh viên, Khoa Sư phạm Khoa học tự nhiên,Trường Sư phạm,

Trường Đại học Đồng Tháp, Việt Nam

[2]Khoa Sư phạm Khoa học tự nhiên,Trường Sư phạm,Trường Đại học Đồng Tháp, Việt Nam

**Tác giả liên hệ, Email: hvphuc@dthu.edu.vn*

Lịch sử bài báo

Ngày nhận: 31/3/2025; Ngày nhận chỉnh sửa: 12/4/2025; Ngày duyệt đăng: 14/4/2025

Tóm tắt

Trong bài báo này, chúng tôi nghiên cứu các trạng thái điện tử theo mô hình đơn hạt của silicene dưới một từ trường giảm theo hàm mũ. Bằng cách giải các phương trình Dirac-Weyl, chúng tôi thu được các biểu thức chính xác cho các hàm sóng và phổ mức Landau tương ứng. Chúng tôi cũng xem xét chi tiết các tác động của điện trường, trường Zeeman và từ trường không đồng nhất lên mật độ xác suất và mật độ dòng xác suất trong silicene. Hơn nữa, chúng tôi so sánh các kết quả của mình với các kết quả tương ứng trong graphene khi có từ trường không đồng nhất.

Từ khóa: *Phương trình Dirac-Weyl, Silicene, Từ trường giảm theo hàm mũ.*

1. Introduction

With the rapid advancement of science and technology, materials science, particularly low-dimensional physics, is attracting increasing research interest (Muoi et al., 2020; Phuc, 2015; Phuc et al., 2015). Among of them, two-dimensional (2D) material systems such as graphene and silicene are receiving special attention. Silicene is a 2D material composed of silicon atoms arranged in a honeycomb lattice, similar to graphene (Oughaddou et al., 2015). Unlike graphene, silicene has a slightly buckled structure due to the larger atomic radius of silicon (Roman & Cranford, 2014). This unique geometry gives silicene remarkable electronic properties, including a tunable bandgap and strong spin-orbit coupling, making it promising for applications in nanoelectronics, spintronics, and valleytronics (Kharadi et al., 2020). Additionally, its compatibility with existing silicon-based technology enhances its potential for future semiconductor devices. Researchers continue to explore silicene's properties and applications, particularly in the development of next-generation electronic components (Chen et al., 2024).

The Landau-level (LL) structure of 2D-materials under an exponentially decaying magnetic field presents a fascinating topic in condensed matter physics (Le et al., 2022). Due to its buckled structure and strong spin-orbit coupling, silicene exhibits unique electronic properties distinct from graphene. When subjected to a non-uniform magnetic field that decays exponentially, the energy spectrum and LLs become highly tunable, leading to interesting quantum phenomena (Hoa et al., 2022). This field configuration influences the behavior of charge carriers, modifying their localization and transport properties. Studying the LL structure in such conditions provides valuable insights into the quantum Hall effect, valley-dependent transport, and potential applications in spintronics and optoelectronics.

To determine the LL structure of 2D systems, scientists typically solve the Dirac equation for the given system (Wang & Jin, 2013). Recently, the supersymmetric (SUSY) method (Ghosh, 2009) has emerged as an effective approach for this purpose. In this work, we use the SUSY method to find the analytical solutions of the Dirac-Weyl equations for the Dirac electron in silicene in the presence of an exponentially decaying magnetic field (EDMF). The behavior of the LL structure, eigenfunctions, probability density, and current density has also been analyzed in detail

2. Model and analytical results

We consider a silicene system oriented in the (*xy*)-plane. The system is placed under an EDMF $\vec{B}(x,y)=(0,0,B(x))$, with

$$B(x)=B_0e^{-x/\lambda} \tag{1}$$

is exponentially decaying in the *x*-direction where λ is the penetration depth of the magnetic field (Wang & Jin, 2013). The vector potential is chosen so that $\vec{A}(x,y)=(0,A_y(x),0)$, where $A_y(x)=-B_0\lambda(e^{-x/\lambda}-1)$. The Hamiltonian of the massless particle near the Dirac point can be described by a two-component Dirac-Weyl equation (Muoi et al., 2020; Shakouri et al., 2014)

$$H_0=v_{\mathrm{F}}(\tau\sigma_x\pi_x+\sigma_y\pi_y)+\Delta_{\tau,s}^{z}\sigma_z+sM_zI_2, \tag{2}$$

where $v_{\mathrm{F}}=5.42\times10^5$ m/s is the Fermi velocity, $\tau=\pm1$ refers to the valley index (for K and K'), σ_i denote the Pauli matrices $(i=x,y,z)$, I_2 is a unit matrix, $\Delta_{\tau,s}^{z}=\tau s\Delta_{\mathrm{SO}}-\Delta_z$ where

$\Delta_{SO} = 3.9$ meV is the spin-orbit interaction strength (Liu et al., 2011), $\vec{\pi} = \vec{p} + e\vec{A}$ is the canonical momentum with $\vec{p} = -i\hbar\vec{\nabla}$ being the normal momentum, $\Delta_z = edE_z$ is a quantity related to the alternating potentials between saturated sublattices, with $2d$ is the distance between them (Ezawa, 2012), and $M_z = e\hbar B(x)/m_e$ is the Zeeman field part with $m_e = 0.26\,m_0$ is the electron effective mass in silicene. The time-independent Dirac-Weyl equation in silicene is written as follows

$$v_F[\tau\sigma_x(p_x + eA_x) + \sigma_y(p_y + eA_y) + \Delta\sigma_z]\psi(x,y) = E\psi(x,y), \tag{3}$$

where the term $\psi(x,y) = \left(e^{ik_y y}/\sqrt{L_y}\right)\psi(x)$ is the two-component eigenfunction with

$$\psi(x) = \begin{pmatrix} \psi_+(x) \\ i\psi_-(x) \end{pmatrix} \tag{4}$$

being the eigenfunction in the *x*-direction, and *i* the units of imaginary numbers. Inserting Eq.(4) into Eq.(3), then using the SUSY method with the effective potential

$$V_\pm(x) = (\hbar v_F)^2\left[W^2 \pm \tau(\partial_x W)\right], \tag{5}$$

where

$$W = k_y + \left(\frac{e}{\hbar}\right)A_y = k_y + \frac{eB_0\lambda^2}{\hbar}\left(1 - e^{-x/\lambda}\right) \tag{6}$$

is the super-potential function, we obtain the following expression for the energy

$$E_{n,p}^{\tau,s} = sM_z + p\sqrt{\left(\frac{\hbar v_F}{\lambda}\right)^2 n(2\xi_0 - n) + (\Delta_{\tau,s}^z)^2}. \tag{7}$$

In Eq.(7), $p = \pm 1$ stands for the conduction and valence bands, respectively, n is an integer denoting the LL index, $\xi_0 = \left(\lambda/\alpha_c(x_0)\right)^2$, where $\alpha_c(x) = \left(\hbar/eB(x)\right)^{1/2}$ is the non-uniform magnetic length and x_0 is the center of orbit, written as follows

$$x_0 = \lambda \ln\left(\frac{eB_0\lambda^2}{\hbar\xi_0^2}\right). \tag{8}$$

The corresponding eigenfunction in Eq.(4) can be written

$$\psi_n(x) = \begin{pmatrix} A_{n,p}^{\tau,s}\phi_{n-1}(x) \\ iB_{n,p}^{\tau,s}\phi_n(x) \end{pmatrix}, \tag{9}$$

Here, the normalization constants are

$$A_{n,p}^{\tau,s} = \sqrt{\frac{\left(E_{n,p}^{\tau,s} - sM_z\right) + \Delta_{\tau,s}^z}{2\left(E_{n,p}^{\tau,s} - sM_z\right)}}, \qquad B_{n,p}^{\tau,s} = \sqrt{\frac{\left(E_{n,p}^{\tau,s} - sM_z\right) - \Delta_{\tau,s}^z}{2\left(E_{n,p}^{\tau,s} - sM_z\right)}}, \tag{10}$$

and the component eigenfunctions

$$\phi_n(x)=\sqrt{\frac{(2\beta)n!\,\bar{\lambda}}{\alpha_c(x_0)(n+2\beta)!}}(2\xi_0)^{\beta}e^{-\beta X\bar{\lambda}}e^{-\xi_0 e^{-X\bar{\lambda}}}L_n^{2\beta}\left(2\xi_0 e^{-X\bar{\lambda}}\right). \tag{11}$$

Here, we denoted $\beta^2=\xi_0^2-\left(\frac{\lambda}{\hbar v_{\mathrm{F}}}\right)^2\left[\left(E_{n,p}^{\tau,s}-sM_z\right)^2-\left(\Delta_{\tau,s}^{z}\right)^2\right]$, $\bar{\lambda}=\alpha_c(x_0)/\lambda=1/\sqrt{\xi_0}$, $X=(x-x_0)/\alpha_c(x_0)$, and $L_n^{2\beta}(x)$ are the *n*-order Laguerre polynomials

3. Numerical results and discussions

Using the relation $\xi=\xi_0 e^{-\bar{\lambda}X}$, we rewrite the effective potentials in Eq. (5) as follows

$$V_{\pm}(x)=\frac{1}{2}\left[\hbar\omega_c(x_0)\right]^2\left[\xi_0\left(1-e^{-X\bar{\lambda}}\right)^2\pm\tau e^{-X\bar{\lambda}}\right]. \tag{12}$$

This has the same form as that obtained in gapped graphene (Le et al., 2022), implying that the effective potential is independent of the system's structure.

For the strong inhomogeneity magnetic field (small λ), the strong asymmetry of the effective potentials is more clear as shown in Fig.1(a). At very large values of *x*, both $V_{\pm}(x)$ reach their saturated value of $\xi_0\left[\hbar\omega_c(x_0)\right]^2/2$. For the weak inhomogeneity magnetic field (large λ or small $\bar{\lambda}$), we have

$$\lim_{\bar{\lambda}\to 0}V_{\pm}(x)=\frac{1}{2}\left[\hbar\omega_c(x_0)\right]^2(X^2\pm\tau). \tag{13}$$

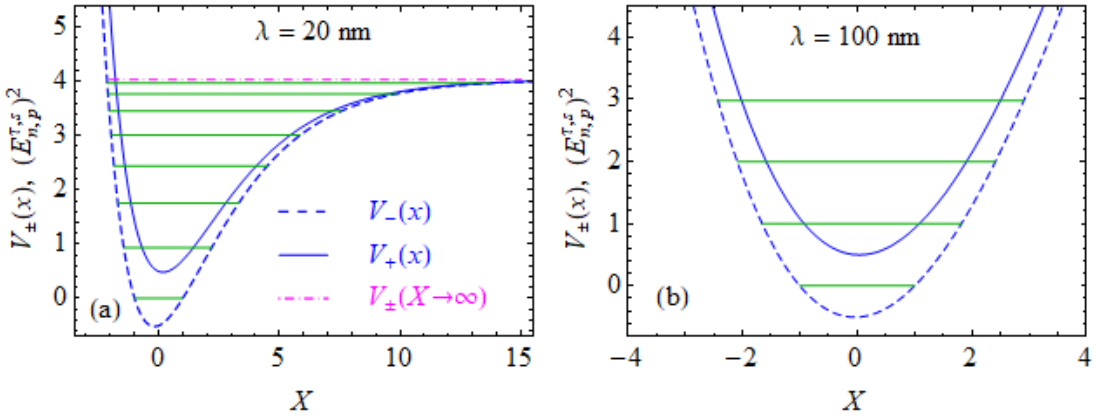

Figure 1. The dependence of the $V_{\pm}(x)$ and E_n on the X-parameter for two values of λ: (a) for $\lambda=20$ nm, and (b) for $\lambda=100$ nm. The results are evaluated at $B=10$ T, $\Delta_z=0$, and $M_z=0$.

This means that in the presence of an EDMF, the system behaves similarly to one under a UMF when the inhomogeneous component is weak (Fig.1(b)). This symmetry indicates that, under certain conditions, $\lambda\geq 100$ nm, the impact of EDMF on the LLs spectrum of silicene closely resembles that of a UMF. Furthermore, since the magnetic field expression in Eq.(1) simplifies to the UMF case when the inhomogeneous term is negligible, it confirms that EDMF can effectively mimic a uniform field. This observation is consistent

with previous studies on graphene (Le et al., 2022), reinforcing the structural and electronic similarities between silicene and graphene. The equivalence in their response to an external magnetic field highlights the fundamental connection between these two materials, suggesting that insights gained from graphene studies may apply to silicene under similar conditions.

Note that, unlike in the case of a UMF (Shakouri et al., 2014), the number of Landau levels (LLs) in the presence of an inhomogeneous magnetic field is limited. This behavior is consistent with the findings for gapped graphene (Le et al., 2022). The total number of LLs, excluding the zero-energy level, being $N_{\max}$, can be found from the condition that $E_n^2 < V_{\pm}(X \to \infty)$, leading to

$$N_{\max} = \left[\xi_0 - \sqrt{\xi_0^2 - 2\xi_0 \left(\left(\frac{\sqrt{\xi_0}}{\sqrt{2}} - \frac{sM_z}{\hbar\omega_c(x_0)} \right)^2 - \left(\frac{\Delta_{\tau,s}^z}{\hbar\omega_c(x_0)} \right)^2 \right)} \right] + 1, \tag{14}$$

where $[...]$ means "the integer part of". For the parameters used in Fig.1(a), we have $N_{\max} = [7.9] + 1$, leading to the fact that there are $(7+1) = 8$ LLs in the energy spectrum, which is shown clearly in Fig.1(a). Similarly, it is also found from Eq. (14) that $N_{\max} = 161$ for the case of $\lambda = 100\,\text{nm}$, which confirms that the EDMF behaves like a UMF in this case.

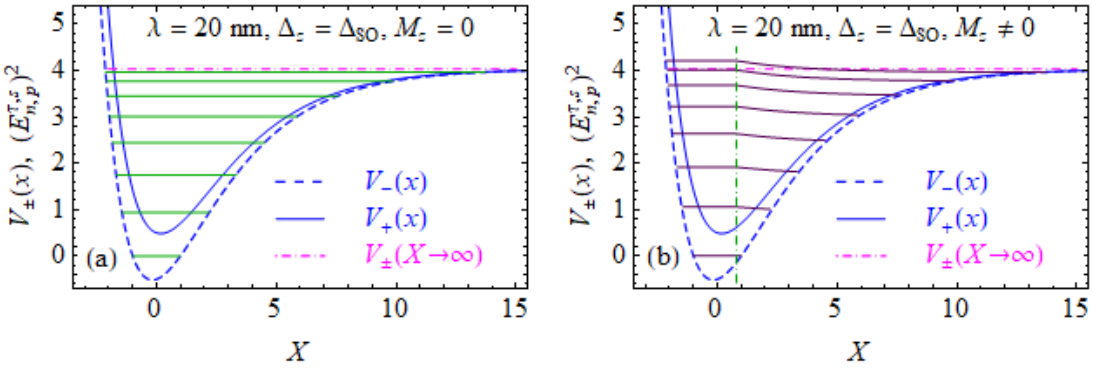

Figure 2. The dependence of the $V_{\pm}(x)$ and E_n on the *X*-parameter for the cases of (a) without and (b) with Zeeman field.

We now examine the effect of an external electric and Zeeman fields on the LL spectrum. As observed in Fig.2(a), both the effective potential and the LL structure remain unchanged compared to the case without an electric field, as shown in Fig.1(a). This indicates that the electric field has a negligible impact on the LL spectrum of silicene.

In Fig.2(b), we show the dependence of the *X*-parameter in the presence of the Zeeman field. It can see that the Zeeman field does not affect the effective potentials but the LLs spectrum. In the small values of *X* such that $x = X\alpha_c(x_0) + x_0$ is negative, the LLs remain unchanged values but have higher values compared to those in the case of the absence Zeeman field show in Fig.2(a). In the range $x \geq 0$, i.e., $X \geq -x_0 / \alpha_c(x_0)$, the LLs start decrease caused by the increase of the Zeeman field, M_z, with *X*. The dashed-dotted vertical

line shows the position of $X = 0.8$ where the LLs start reducing. We can easily check that with the parameters used in Fig.3, from Eq.(8), we have: $-x_0 / \alpha_c(x_0) = 0.8$.

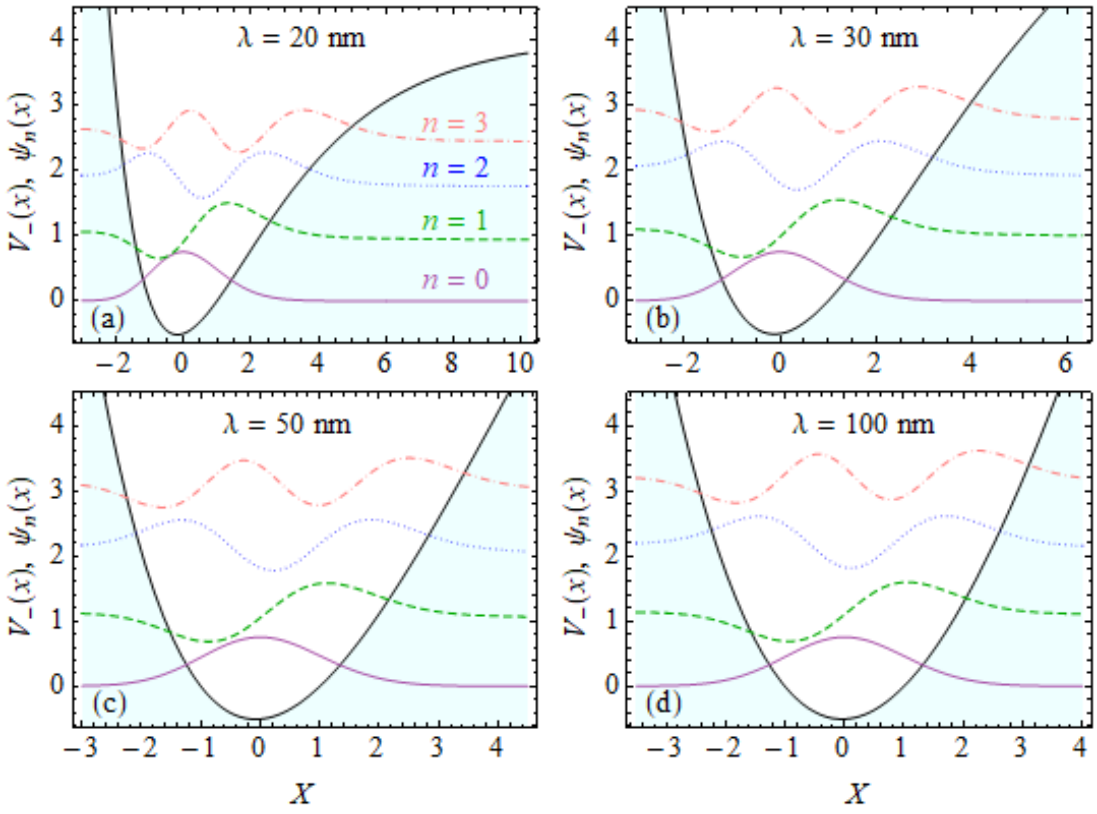

Figure 3. The first four wave functions in silicene in the presence of electric and Zeeman fields for different values of λ.

Now, let us examine the behavior of wave functions under different magnetic field conditions. In Fig.3, we present four first-order wave functions of an electron in silicene for two different values of the non-uniform magnetic length scale λ. It is evident that in the case of an EDMF with $\lambda = 20\text{nm}$, the wave functions exhibit noticeable asymmetry. In contrast, when subjected to a UMF with $\lambda = 100\text{nm}$, the wave functions almost remain symmetric. This asymmetry observed in the EDMF case can be attributed to the dependence of the effective potential $V_{\pm}(X)$ on the parameter λ, as illustrated in Fig.1. Specifically, for small values of λ, the inhomogeneous nature of the field becomes more pronounced, leading to an asymmetric distribution of the wave functions. However, in the UMF case, where λ is significantly larger as shown in Fig.3(d) with $\lambda = 100\text{nm}$, the system effectively experiences a uniform field, resulting in symmetric wave functions. These findings emphasize the crucial role of the non-uniform magnetic field in shaping the quantum states of silicene. The ability to control wave function symmetry by tuning λ could have essential implications for silicene-based quantum devices, particularly in applications requiring precise manipulation of electron states.

We now turn our attention to study the probability density and probability current density. The probability density and probability current density for the first few quantum states under a strong inhomogeneous magnetic field $(\lambda = 20\text{nm})$ are depicted in Fig.4. The

probability density distributions are obtained using the following expression

$$\rho_n(x) = \psi_n^{\dagger}(x)\psi_n(x), \tag{15}$$

where $\psi_n(x)$ represents the eigenfunctions given in Eq.(11), and $\psi_n^{\dagger}(x)$ denotes their Hermitian conjugate. This function describes the likelihood of finding an electron at a given position X. Meanwhile, the probability current density, which characterizes the flow of probability per unit time per unit area, is determined by

$$J_n(x) = ev_{\mathrm{F}}(\psi_{n-1}^{*}\psi_n + \psi_n^{*}\psi_{n-1}). \tag{16}$$

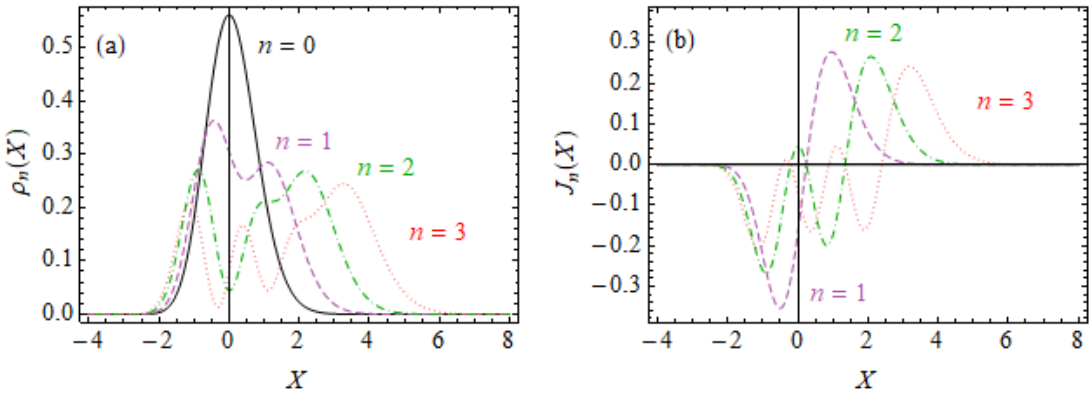

Figure 4. The dependence of the probability density, $\rho_n(X)$, and the probability current density, $J_n(X)$, on the *X*-parameter in the presence of electric and Zeeman fields at $\lambda = 20$ nm.

From Fig.4(a), we observe that for the ground state ($n = 0$), the probability density distribution is symmetric and reaches its peak at $X = 0$. This indicates that an electron in the $n = 0$ state is most likely to be found at the center of the system. Moreover, the symmetry or asymmetry of the probability density distributions for higher quantum states $(n > 0)$ directly corresponds to the symmetry properties of their respective eigen-functions, as depicted in Fig.3. Specifically, when λ is small the effective potential exhibits asymmetry, leading to an asymmetric probability distribution. These findings align well with previous studies on gapless graphene (Le et al., 2022).

Regarding the probability current density, Fig.4(b) demonstrates that $J_0(X) = 0$, implying that the zero-state does not contribute to current flow. This result is expected, as a fully symmetric ground-state wave-function does not generate a directional current. However, for $n = 1, 2, 3,$ the probability current density shifts to the right as the LL index increases, a consequence of the asymmetric effective potential under strong inhomogeneous magnetic fields. This behavior mirrors that of the probability density distributions in Fig.4(a), reinforcing the idea that the asymmetry in probability flow stems directly from the asymmetry in the eigenfunctions, as depicted in Fig.3(a).

Furthermore, the observed shift in the probability current density for higher Landau levels $(n > 0)$ suggests that the inhomogeneous magnetic field plays a crucial role in modifying electron transport properties in silicene. As the LL index increases, the probability current density becomes more pronounced, indicating more substantial electron localization

effects in regions with asymmetric potential landscapes. This behavior is particularly significant in nanoscale electronic devices, where external fields can be used to manipulate electron flow for practical applications. Additionally, the similarity between the probability density and current density distributions in silicene and gapless graphene highlights the universality of these effects across different Dirac materials. Despite subtle differences in spin-orbit coupling and sublattice asymmetry, the fundamental influence of inhomogeneous magnetic fields on the quantum states of charge carriers remains consistent. These findings not only reveal the fundamental behavior of studying optical transitions in silicene but also offer valuable insights into the tunability of electronic states, which is a key requirement for functional device integration. The demonstrated control of the Landau levels spectrum through external magnetic fields suggests that silicene's electronic states can be precisely modulated in real time.

4. Conclusion

In summary, our findings provide deeper insights into the role of inhomogeneous magnetic fields in tailoring the electronic properties of silicene. The dependence of the Landau level structure on the penetration depth suggests potential applications in designing tunable electronic and optoelectronic devices. By carefully controlling the magnetic field profile, one can engineer specific quantum states, which may be beneficial for developing novel quantum transport phenomena in silicene-based systems. Additionally, the asymmetry observed in the probability density and current density distributions highlights the significant impact of the effective potential on electron localization. This effect could be further explored in the context of valleytronics, where controlled manipulation of electronic states is crucial for information processing. Future studies on the interaction between inhomogeneous magnetic fields and external perturbations, such as electric fields or strain, could provide a more comprehensive understanding of silicene’s electronic behavior and broaden its applicability in next-generation nanoelectronic devices.

Acknowledgements: This research is supported by the project SPD2024.02.21.

References

Chen, L., Zhang, S., Duan, Y., Song, X., Chang, M., Feng, W., & Chen, Y. (2024). Silicon-containing nanomedicine and biomaterials: materials chemistry, multi-dimensional design, and biomedical application. *Chemical Society Reviews*, *53*(3), 1167-1315. https://doi.org/10.1039/D1CS01022K

Ezawa, M. (2012). Spin-valley optical selection rule and strong circular dichroism in silicene. *Physical Review B*, *86*(16), 161407. https://doi.org/10.1103/PhysRevB.86.161407

Ghosh, T. K. (2009). Exact solutions for a Dirac electron in an exponentially decaying magnetic field. *Journal of Physics: Condensed Matter*, *21*(4), 045505. https://doi.org/10.1088/0953-8984/21/4/045505

Hoa, L. T., Phuong, L. T. T., Kubakaddi, S. S., Hieu, N. N., & Phuc, H. V. (2022). Landau levels and magneto-optical responses in Weyl semimetal quantum wells in a non-uniform magnetic field. *Physical Review B*, *106*(7), 075412. https://doi.org/10.1103/PhysRevB.106.075412

Kharadi, M. A., Malik, G. F. A., Khanday, F. A., Shah, K. A., Mittal, S., & Kaushik, B. K. (2020). Review—Silicene: From Material to Device Applications. *ECS Journal of Solid State Science and Technology*, *9*(11), 115031. https://doi.org/10.1149/2162-8777/abd09a

Le, T. H., Tran, N. B., Nguyen, N. H., Le, T. N. T., & Huynh, V. P. (2022). Dirac electron in gapped graphene under exponentially decaying magnetic field. *Tạp chí Khoa học Đại học Đồng Tháp*, *11*(5), 35-40. https://doi.org/10.52714/dthu.11.5.2022.978

Liu, C.-C., Jiang, H., & Yao, Y. (2011). Low-energy effective Hamiltonian involving spin-orbit coupling in silicene and two-dimensional germanium and tin. *Physical Review B*, *84*(19), 195430. https://doi.org/10.1103/PhysRevB.84.195430

Muoi, D., Hieu, N. N., Nguyen, C. V., Hoi, B. D., Nguyen, H. V., Hien, N. D., Poklonski, N. A., Kubakaddi, S. S., & Phuc, H. V. (2020). Magneto-optical absorption in silicene and germanene induced by electric and Zeeman fields. *Physical Review B*, *101*(20), 205408. https://doi.org/10.1103/PhysRevB.101.205408

Oughaddou, H., Enriquez, H., Tchalala, M. R., Yildirim, H., Mayne, A. J., Bendounan, A., Dujardin, G., Ait Ali, M., & Kara, A. (2015). Silicene, a promising new 2D material. *Progress in Surface Science*, *90*(1), 46-83. https://doi.org/10.1016/j.progsurf.2014.12.003

Phuc, H. V. (2015). Nonlinear optical absorption via two-photon process in $GaAs/Ga_{1-x}Al_xAs$ quantum well. *Journal of Physics and Chemistry of Solids*, *82*, 36-41. https://doi.org/10.1016/j.jpcs.2015.03.004

Phuc, H. V., Hieu, N. N., Dinh, L., & Phong, T. C. (2015). Nonlinear optical absorption in parabolic quantum well via two-photon absorption process. *Optics Communications*, *335*, 37-41. https://doi.org/10.1016/j.optcom.2014.09.004

Roman, R. E., & Cranford, S. W. (2014). Mechanical properties of silicene. *Computational Materials Science*, *82*, 50-55. https://doi.org/https://doi.org/10.1016/j.commatsci.2013.09.030

Shakouri, K., Vasilopoulos, P., Vargiamidis, V., & Peeters, F. M. (2014). Spin- and valley-dependent magnetotransport in periodically modulated silicene. *Physical Review B*, *90*(12), 125444. https://doi.org/10.1103/PhysRevB.90.125444

Wang, D., & Jin, G. (2013). Effect of a nonuniform magnetic field on the Landau states in a biased AA-stacked graphene bilayer. *Physics Letters A*, *377*(40), 2901-2904. https://doi.org/10.1016/j.physleta.2013.08.041